Journal of Crystal Growth 603 (2023) 126978

Contents lists available at ScienceDirect

Journal of Crystal Growth

journal homepage: www.elsevier.com/locate/jcrysgro

The transformation of amorphous calcium carbonate to calcite and classical nucleation theory

C.L. Freeman *, J.H. Harding

Department of Materials Science and Engineering, University of Sheffield, Mappin Street, Sheffield S1 3JD, United Kingdom

ARTICLE INFO

Communicated by James J. De Yoreo

Keywords:
A1 Interfaces
A1 Computer simulation
A1 Supersaturated solutions
A2 Growth from solutions
B1 Minerals
B1 Calcium compounds

ABSTRACT

The interfaces of calcite with water, dehydrated and hydrated amorphous calcium carbonate are studied with molecular dynamics simulations. The interfacial energies demonstrate that the calcite interface is most stable when in contact with water or low concentration solutions rather than amorphous calcium carbonate. These values are used to test the interplay between supersaturation and the interfacial energy for calcite. They demonstrate that a dissolution-reprecipitation process should always be energetically preferred to a solid state transformation of amorphous calcium carbonate to calcite.

1. Introduction

There is a large (and still growing) literature on the possible mechanisms by which calcium carbonate crystals are produced from a supersaturated solution. Depending on the authors and the experimental conditions, prenucleation (nanometre-sized) clusters [1,2], dense liquid phases [3] solid amorphous clusters of various sizes and compositions [1], crystalline particles [4] and spinodal decompositions [5] have been invoked either singly or in combination to give a multi-step pathway. These varied mechanisms may coexist; the dominating mechanism depending on conditions. Studies [6] on the solution speciation at mild supersaturation suggest that the solution contains free cations and anions (CO_3^{2-} and/or HCO_3^- depending on the conditions) and a limited population of larger ion clusters that are formed by density fluctuations in the solution, consistent with classical nucleation theory [7]. On the other hand, it has been claimed that these larger clusters are thermodynamically stable and, with increasing supersaturation, can aggregate to form an amorphous phase [8] which is usually hydrated. This can then convert to one of the calcium carbonate polymorphs (usually calcite or vaterite; aragonite can also be formed in the presence of suitable additives [1]). The formation of other less stable phases before formation of the final stable solid phase (Ostwald's law of stages) is common in solution-based nucleation [9]. The formation of these phases means that we are altering the supersaturation of our system by depleting ions. The conversion of these early phases to our final stable phase may proceed by various mechanisms. For $CaCO_3$ the majority of authors have reported that the conversion process of the ACC phase to calcite (or other polymorphs) proceeds by either a dissolution, reprecipitation processes [10–13] or nucleation on the surface of precursor phases [14]. The assumption is that the supersaturation reduces during growth of the ACC phase and that this ultimately leads to instability of the ACC phase and its dissolution providing the opportunity for formation of a more stable crystalline phase. The majority of reports of a solid state transformation presume direct dehydration of bulk ACC [15–18] but there are also cases involving aggregation of nanoparticles [19,20] and hetero-nucleation at surfaces [21]. These all suggest that the ACC phase may also interconvert without dissolution. This raises the question - under what conditions is a dissolution reprecipitation process preferred to a solid state transition?

Unless the polymorph formed is ikaite or calcium carbonate monohydrate a solid state transformation requires the expulsion of water. This process is generally thought to involve a high energy barrier although the debate continues as to whether it is thermodynamic or kinetic in origin [17,22]. Albéric *et al* [22] argue strongly for the importance of water in the stabilisation of ACC. Although the transformation enthalpy from ACC to calcite has a linear correlation with the water content, the free energy of transformation is independent of this from the anhydrous case to a composition of $CaCO_3{\cdot}1.3H_2O$ (a mole fraction of 57% water). This is ascribed to a countervailing entropy term. Water undoubtedly has a strong effect on the ion mobility. Both advanced experimental

* Corresponding author.
E-mail address: c.l.freeman@sheffield.ac.uk (C.L. Freeman).

https://doi.org/10.1016/j.jcrysgro.2022.126978
Received 14 June 2022; Received in revised form 21 October 2022; Accepted 4 November 2022
Available online 8 November 2022

characterisation techniques [1,18,23] and molecular dynamics simulations [24] show that there are two states of water in ACC, "mobile" and "rigid" and the ratio between them controls both the degree of order in ACC and its stability against crystallisation [25]. The synthesis conditions are likely to control this ratio.

Whatever pathway the formation of calcite follows, at some point the new, separate phase must form an interface with the surrounding medium. This process can be understood from the viewpoint of classical nucleation theory. There are many extended reviews of classical nucleation theory (CNT) e.g. [9,26–28], so it is not necessary to give more than a brief outline here. The earliest forms of CNT confined themselves to the formation of a condensed phase from its vapour. It was assumed that the condensed phase was favoured over the vapour phase under the conditions of the experiments, giving a chemical potential driving force arising from the difference between the bulk free energy of the condensed phase and that of the vapour. This driving force has to overcome the free energy penalty associated with the formation of an interface between the condensed and vapour phases and depends on the nature of the interface formed. The nucleus is treated as a macroscopic object, with a size-independent chemical potential. Similarly, the interface is presumed to be a single interface and any effects of nucleus size or faceting are ignored. When this approach was extended to the precipitation of a solid from solution, the partial pressure (strictly speaking the fugacity) of the vapour was replaced by the activity of the solute in solution. The change in chemical potential between a species in a homogeneous solution of a given activity and the chemical potential of the condensed phase (assumed to be size-independent) is the supersaturation of the species in solution and represents the driving force of phase separation of the solute from the solvent. This model introduces further complications. In solutions, except in the ideal case of infinite dilution, the activity is not always well approximated by the concentration. Also, when an interface is present the local solute concentrations close to it may differ from the bulk [29]. This may produce a different interfacial energy to that expected at the concentration and also one which will could vary during the nucleation process as the ion concentration varies.

In the basic version of CNT, the nucleation rate, *J*, (i.e. the number of thermodynamically stable nuclei formed per unit volume of solution) is given by

$$J = A_{kin} exp(-\Delta G_c/kT) \tag{1}$$

where A_{kin} is a kinetic prefactor and ΔG_c is the free energy barrier to the formation of a nucleus that will grow without limit to form a macroscopic crystal. For a spherical nucleus we can write a general expression for the free energy

$$\Delta G = -\frac{4}{3}\pi r^3 \Delta\mu + 4\pi r^2 \gamma \tag{2}$$

where r is the radius of the nucleus, $\Delta\mu$ is the change in chemical potential between solution and bulk solid and can be written as

$$\Delta\mu = kTln\left(\prod a_i/K_{sp}\right) \tag{3}$$

where a_i are the activities of dissolved components of the molecular formula unit of the crystal and K_{sp} is the product of the activities of those components when the solution is in equilibrium with the bulk crystal. γ is the interfacial energy. Differentiation of equation (1) gives the thermodynamic barrier to nucleation, ΔG_c,

$$\Delta G_c = f\gamma^3\Omega^2/(\Delta\mu)^2 \equiv f\gamma^3\Omega^2/k^2T^2\sigma^2 \tag{4}$$

where the supersaturation, $\sigma = ln(\prod a_i/K_{sp})$. f is a shape factor which for a spherical nucleus is equal to $16\pi/3$, Ω is the molar volume of the structural unit added to the cluster. From equation (4) it is clear that CNT suggests that the change in free energy of growing nuclei is dominated by interfacial energies at small sizes. Nuclei with relatively low interfacial energies are more likely to grow beyond a critical size, where continued growth becomes spontaneous.

A_{kin} depends on the mechanism whereby the structural unit goes from the bulk solution to attachment to the growing nucleus. The kinetic factor is given by [30–32]

$$A_{kin} = \sqrt{\frac{\gamma}{kT}}\left(\frac{kT}{hR^2}\right) exp(-\Delta G_A/kT) \tag{5}$$

where h is Planck's constant, R the radius of the critical nucleus and ΔG_A the activation free energy of the process of transferring a structural unit of the nucleus from the solution to the nucleus. If A_{kin} is dominated by the process of diffusion of the mobile species in solution, it can be approximated by $A_{kin} \approx D/\Omega^{5/3}$ where D is the diffusion coefficient of the species in water. A_{kin} is of the order of 10^{39} $m^{-3}s^{-1}$

In this paper we attempt to understand the interface between calcite and ACC (or a highly saturated water precursor). Assuming the formation of calcite will occur from a solution or an ACC phase, then by examining this interface and determining the interfacial energy we can comment on calcite nucleation. Our study allows us to examine the role of supersaturation variation at the nucleating crystal interface through a classical nucleation theory interpretation.

2. Methods

All molecular dynamics simulations were performed using DLPOLY Classic [33] with a timestep of 0.5 fs. Forcefield terms were taken from Raiteri *et al* [34]. Three-dimensional simulation supercells with periodic boundary conditions containing an interface between calcite and hydrated amorphous calcium carbonate (*h*-ACC) were constructed for different compositions of *h*-ACC using the following procedure. Calcite slabs exposing the (10.4) surface of 576 formula units were built with an approximate surface area of 2650 $Å^2$ for each surface. Simulation cells of *h*-ACC were then made using the PACKMOL package [35] with approximately 1200 H_2O + $CaCO_3$ units for mole fractions of $CaCO_3$ of 0.005, 0.01, 0.03, 0.05, 0.1, 0.15, 0.2, 0.3, 0.4 0.5, 0.6, 0.7, 0.8 0.9 and 1.0. Table S1 in the appendix lists the specific atom numbers for each simulation. Following a similar procedure to Malini et al, the ACC cells were heated to 3000 K in steps of 300 K (i.e. 300 K, 600 K, 900 K etc) for 0.5 ns under a NVT ensemble. These were then maintained at 3000 K for 2 ns. The cells were then quenched back down to 300 K in steps of 300 K for 250 ps. These cells were then relaxed using a NPT Nosé-Hoover ensemble (0.01 ps thermostat and 0.05 ps barostat relaxation times respectively) at a pressure of 0 atm and a temperature of 300 K. After relaxation each cell was joined to a (10.4) calcite slab to make the final simulation supercell (see Fig. 1). The supercells were then equilibrated at 0 atm. and 300 K until convergence was achieved in energy and volume (typically this required 2–3 ns). Three different configurations were run for each solution composition and the configuration of lowest energy was selected for further analysis. The variation in interfacial energy between the lowest and highest interfaces is listed in Table S1. The interfacial energy, γ, is the energy of the calcite *h-ACC* interface with respect to bulk pure calcite and bulk *h*-ACC (i.e. not a cleavage energy). It was therefore calculated using

$$\gamma = \frac{E_{calcite\backslash h-ACC} - bE_{calcite} - E_{h-ACC}}{2A} \tag{6}$$

where $E_{calcite\backslash h\text{-}ACC}$ is the configurational energy of the simulation supercell with the calcite *h*-ACC interface. $E_{calcite}$ is the configurational energy of the same number of formula units (*b*) of calcite as present in the simulation supercell and $E_{h\text{-}ACC}$ is the configurational energy of the relaxed cell of hydrated ACC. *A* is the area of the interface between calcite and *h*-ACC.

We use our calculated values of γ combined with literature values [4] in equation (4) to calculate the barrier to nucleation at several supersaturation values. Alternatively, when considering a solid state transformation and nucleation rather than solution based nucleation, the supersaturation, σ, can be replaced with the free energy difference

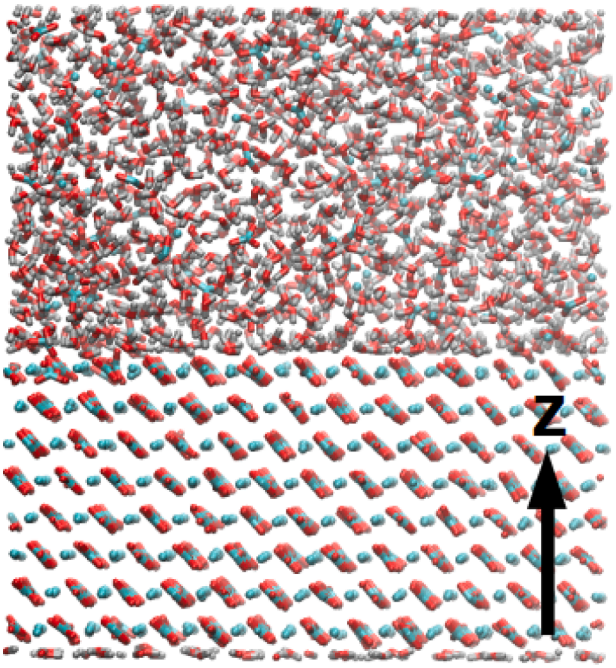

Fig. 1. Simulation cell for interfacial calculations showing z-axis definition for the other Figures. Oxygen (red), carbon (blue), calcium (blue), hydrogen (grey). (For interpretation of the references to colour in this figure legend, the reader is referred to the web version of this article.)

between the phases where $k_B^2T^2\sigma^2$ is replaced with ΔG^2. The energy change for ACC - calcite is taken from a calculation of the mixing configurational energy of calcite and ACC,

$$\Delta E = nE_{calcite} + mE_{water} - E_{ACC(nCaCO_3+mH_2O)} \quad (7)$$

where $E_{calcite}$ is the energy per formula unit of bulk calcite, E_{water} is the energy of a single water molecule taken from a bulk water simulation and $E_{ACC}(n,m)$ is the energy of a hydrated ACC with a molecular composition of n $CaCO_3$: m H_2O. The entropic component of the free energy is assumed to be dominated by the change in the configurational and librational entropy of the water molecules as they transition from the solid state ACC to a liquid phase, ΔG_{water}. There have been several attempts to calculate this value and we used that produced by Rateri *et al* [34] of 42.3 $Jmol^{-1}$ K^{-1} per water molecule. Note this is an estimated value based around a 50:50 mix of $CaCO_3$:H_2O and would not be expected to be constant across the full mixing range as the water environments will vary. The final free energy change is:

$$\Delta G \approx \Delta E + m\Delta G_{water} \quad (8)$$

3. Results and Discussion

Fig. 2 shows the variation of the energy of the calcite *h*-ACC interface as a function of the mole fraction of $CaCO_3$, x_{CaCO_3}, in the *h*-ACC. These clearly show that the interfacial energy is lowest for very low mole fractions of $CaCO_3$ ($x_{CaCO_3} \leq 0.05$) with values less than 0.03 Jm^{-2}. As the mole fraction of $CaCO_3$ increases the interfacial energy increases up to 0.4 Jm^{-2} at $x_{CaCO_3} = 0.5$ - close to a $CaCO_3$:H_2O ratio of 1:1). Beyond this point the interfacial energy fluctuates but remains higher than for the low mole fraction region (even fully dehydrated *h*-ACC ($x_{CaCO_3} = 1$) gives an interfacial energy of 0.22 Jm^{-2}). This suggests that there might be little variation in the interfacial energy of a growing crystal for supersaturations that might be expected within a typical experimental solution. Hence the difference between the local supersaturation (i.e. accounting for the fluctuations caused by surfaces, non-perfect mixing and natural variation) and the average bulk supersaturation may not

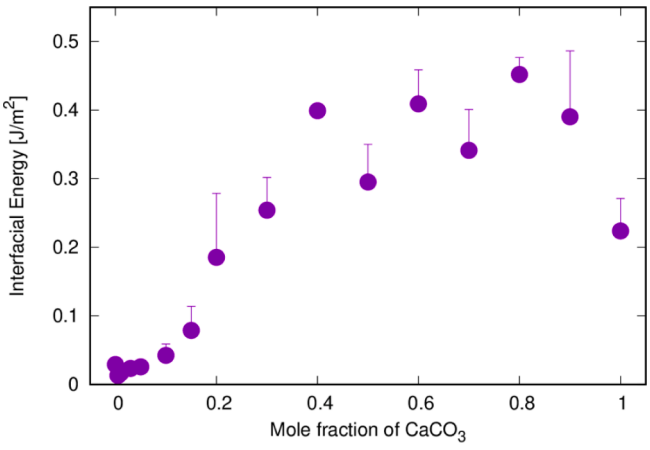

Fig. 2. Interfacial energy of calcite (10.4) surface with *h*-ACC for $0 < x_{CaCO_3} < 1$. Error bar shown covers the range between the minimum value calculated for the three configurations (purple circle) and the maximum value for the three configurations (top of the error bar). (For interpretation of the references to colour in this figure legend, the reader is referred to the web version of this article.)

affect the interfacial energy significantly. However it will still play an important role as the driving force for nucleation and altering the density of ions in the solution volume. Comparison between the three different configurations for each composition is listed in supplementary Table S1 and the effect is shown in Fig. 2. These show the average variation between the three configurations is 0.03 Jm^{-2}. The variation is larger for the higher $CaCO_3$ mole fraction systems which can be understood by the slower dynamics of these systems which means the final energy will be more dependent on the starting configurations. The largest variation is 0.1 Jm^{-2} for $x_{CaCO_3} = 0.9$. The trends remain the same even with the variation and the low $CaCO_3$ mole fraction systems have consistently lower interfacial energies than the medium to high $CaCO_3$ mole fraction systems.

The interfacial energy calculated in this study is only a configurational energy and does not include the entropic component. This component will be primarily associated with the loss of entropy from the water being organised at the calcite surface and therefore we would expect the interfacial free energy to be larger than the values we present here. Calculating this value is a complex process and beyond the remit of this study but previous attempts on water-calcium sulphate interfaces have produced values up to ~ 0.1 Jm^{-2} [36]. Given the same Ca ions are present we would expect similar values and therefore though there could be some variation in this entropic component with the concentration of the solution as well but we would not expect the component to be so large as to change the effective order of the interfacial energies calculated.

Cleaving the calcite surface creates under-coordinated ions in the surface plane. This under-coordination is potentially reduced by interaction with another condensed phase at the interface helping to stabilise the surface and lower the interfacial energy. This effect can be observed in Fig. 3(a) which shows the Z-density profile of the oxygen atoms in the water molecules, O_{water}, in the *h*-ACC with respect to the interface. Previously, it has been shown that the water molecules align with the surface, helping to satisfy the under-coordination of the ions on the calcite side [37,38]. This alignment deteriorates as x_{CaCO_3} increases. At $x_{CaCO_3} = 0.005$ the first peak is sharp and there is a second peak. For $x_{CaCO_3} = 0.2$ the first peak is significantly broader and shorter and the second peak has almost vanished. The CO_3 ions in the *h*-ACC system are able to bind at this under-coordinated interface as the mole fraction of $CaCO_3$ increases within the *h*-ACC to mitigate some of this effect but the structuring of the CO_3 ions is not as well organised and breaks up the inter-water interactions that further stabilise the surface water layers.

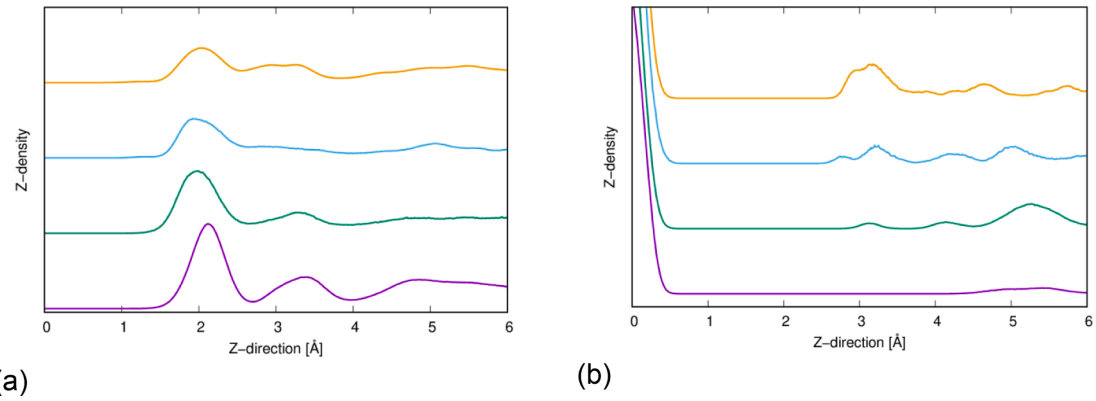

Fig. 3. Z-density profiles of species in *h*-ACC. The Z-direction (ordinate in the graphs) is the normal to the calcite *h*-ACC interfacial plane (the origin is in the plane of the calcite slab closest to the interface) for (a) O_{water} in *h*-ACC. And (b) Ca ions in *h*-ACC.. Colours refer to *h*-ACC compositions: $x_{CaCO_3} = 0.005$ (purple); $x_{CaCO_3} = 0.05$ (green); $x_{CaCO_3} = 0.1$ (blue); $x_{CaCO_3} = 0.2$ (orange). Lines are vertically offset to make them visually clearer. (For interpretation of the references to colour in this figure legend, the reader is referred to the web version of this article.)

In Fig. 3(b) the Z-density profile for the Ca^{2+} ions in *h*-ACC is plotted. At low mole fraction ($x_{CaCO_3} = 0.005$) there are no Ca^{2+} ions near the interface due to their low concentration. At $x_{CaCO_3} \geq 0.05$ the Ca^{2+} ions sit approximately 3.0–3.5 Å from the surface which places them either between the two water layers or within the second one. These ions generate strong solvent shells that structure the surrounding water molecules, preventing them from organising at the calcite surface. This leads to the disruption of the water structure observed for $x_{CaCO_3} = 0.2$ and $x_{CaCO_3} = 0.3$. At higher mole fractions they create an amorphous system of low mobility (due to the strong interactions) preventing the water molecules from reorganising with respect to the surface. This explains why the energy of the calcite:*h*-ACC interface increases as x_{CaCO_3} increases as the water is no longer able to satisfy the under-coordination of the ions that are part of the calcite structure.

Our simulation results suggest that the penalty to nucleus formation arising from the interface energy (γ) will be smallest for solutions with a low value of x_{CaCO_3} (which corresponds to the smallest supersaturation and driving force towards nucleation). Conversely a high supersaturation will correspond to a large interfacial energy, increasing ΔG_c. Therefore we have a potentially interesting case where the two main factors are working against each other. Our observations also suggest that the interfacial energy will lower as ions are depleted from the solution surrounding the nuclei. In an extreme case where local supersaturation decreases substantially this could stabilise a growing nucleus of calcite but in a system with the opposite trend (i.e. increasing interfacial energy with decreasing concentration) we could see a destabilisation of the nucleus which could further inhibit the process.

Although it is possible that different nuclei and other species may exist before the formation of calcite in the system, if we are to form a calcite crystal then at some point we must form a calcite surface and this surface will be in contact with water or a ACC based phase. We are essentially assuming that the nucleus will adopt the equilibrium morphology of the calcite crystal and the surfaces will have an interfacial energy comparable to the infinite surface. Therefore the interfacial energy of that calcite surface will be a barrier on the pathway and will constrain the rate of formation. Since the (10.4) surface has a much lower energy than any other surface, it is likely to be the preferred surface. The differences may appear quite small in Fig. 2 but these are very significant since the nucleation rate depends exponentially on the cube of the interfacial energy. In Fig. 4(a) we have used equation (4) to calculate ΔG_c at a range of compositions and supersaturations in terms of k_BT (values not calculated in this paper were taken from Hu *et al* [4]). The values imply that the barrier to the formation of a calcite nucleus will be much larger from a highly concentrated solution than from a dilute solution.

Alternatively to using arbitrary supersaturations, we can calculate the approximate supersaturation that relates to the actual solution concentration of the interface represented by our hydrated ACC phase and use this value (Fig. 4(b) – purple squares). These will be very large supersaturations as the molality of the solution (see supplementary Table S1) are very large and could provide the extra driving force needed to overcome the large energy barriers associated with the

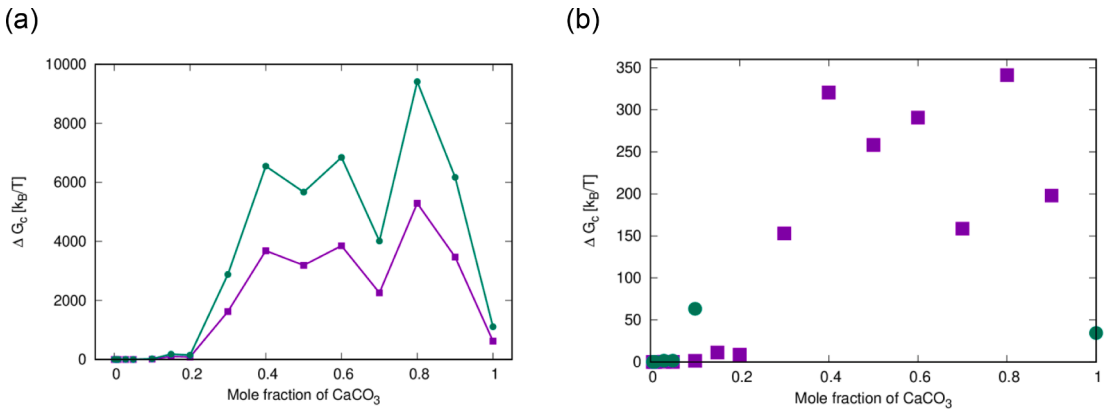

Fig. 4. Critical nucleation barrier, ΔG_c, to the formation of calcite with an interface of *h*-ACC with differing mole fractions of $CaCO_3$ for (a) Supersaturation 3 (green circles), 4 (purple squares) and (b) supersaturation directly approximated to the mole fraction (purple squares) or using a driving force calculated from the free energy difference between the ACC phase and calcite (green circles). (For interpretation of the references to colour in this figure legend, the reader is referred to the web version of this article.)

interfacial energy. These larger supersaturations do lower all the barriers significantly so values become ~ 1 kT for $0 < x_{CaCO_3} < 0.1$, rising to ~ 10 kT at $0.1 < x_{CaCO_3} < 0.2$ and then larger still. Although the barriers are reduced by the very high supersaturations at the high $CaCO_3$ mole fractions these are still an order or orders of magnitude larger for $x_{CaCO_3} > 0.1$.

At the high mole fractions of $CaCO_3$ it can be argued that the system is not a solution and we should consider this as a solid state phase change instead. Calculation of the diffusion coefficients for the water molecules and ions suggests this transition occurs around . $x_{CaCO_3} > 0.3$ (see supplementary table S2). For this purpose we can calculate the free energy differences between the ACC and calcite phases and use this as our driving force (in a similar appraoach to that used in calculations around metal phase transitions e.g. [39,40]). Calculating this free energy is not a trivial set of simulations and we approximate the value by taking the bulk energetic (configurational) differences between the ACC phase and calcite and water, the entropic contribution is assumed to be most dependent on the liberation of water from the ACC phase and we use the value proposed by Rateri *et al* [34] of 42.3 $Jmol^{-1}K^{-1}$. Further details are listed in the methods section. The green circles of Fig. 4(b) shows ΔG_c calculated using these values. As can be seen most of the values are far higher to those taken using supersaturation and therefore sit off the plot. The full range of values (using a natural log plot) can be seen in supplementary material; Figure S1.

Using three different values to the driving force for classical nucleation we observe in all cases that the large interfacial energies associated with higher $CaCO_3$ content dominate and make nucleation with these interfaces present very unlikely. This suggests that a calcite nucleus will struggle to form if surrounded by an ACC phase. Conversely the formation of a calcite nucleus in water will have to overcome a much smaller barrier as the water molecules stabilise the surfaces.

These results agree well with the commonly reported dissolution of ACC followed by re-precipitation of calcite. Hydrated ACC is often observed to be very stable but dehydrated ACC has also been reported with long lifetimes when kept in low humidity environments. Ihil *et al* [15] showed that ACC trapped within a lipid bilayer was stable for very long times. While the lifetime of ACC was shown to alter with the humidity of the air environment [18]. Without the presence of surface water any calcite nucleus would be forced to form within the ACC and therefore its surfaces would be in direct contact with the ACC generating a large barrier to formation as we have calculated and shown in Fig. 4a and 4b. Many solid state transformations are observed via heating and dehydration [15,16,22] which agrees with the large barriers calculated here suggesting that a large amount of heat energy must be added to enable the process. In solution we would note that the transformation process could occur at the surface of the ACC particle as was observed in liquid-cell TEM (forming aragonite) [14] where the crystal phase remained in contact with the ACC particle throughout the nucleation and growth process. By growing on the surface of the ACC particle the majority of the crystal phase will be exposed to the water solution where the interfacial energy is low overcoming the energy penalty of the interface with the ACC. The solid state transformation reported by Walker *et al* [19] and Puget *et al* [20] observed crystalline particles in contact with the ACC which could potentially have been on the surface rather than formation of calcite within the ACC particle as this cannot be easily determined via the electron microscopy methods employed.

The rate of nucleation is a product of the kinetic prefactor term (with units of structural units per m^3s^{-1}) and an exponential term describing effect of the barrier to nucleation. Considering these two terms together in the light of the results in Fig. 2, it is clear that the formation of a calcite nucleus at the surface of ACC, nearby to ACC (where ion concentrations are higher) or immediately following ACC dissolution (again leading to high ion concentrations in the surrounding solution) and growth into the solution ensures the highest rate of nucleation. This system will have a high activity, the lowest thermodynamic barrier and a high concentration of growth species. Combining this understanding we can see that many of the different mechanistic cases reported for the formation of calcite with an ACC precursor can be entirely commensurate with each other and a simple CNT interpretation and understood from a viewpoint of interfacial energies.

CRediT authorship contribution statement

C.L. Freeman: Conceptualization, Data curation, Formal analysis, Funding acquisition, Investigation, Methodology, Project administration, Resources, Software, Supervision, Validation, Visualization, Writing – original draft, Writing – review & editing. **J.H. Harding:** Conceptualization, Formal analysis, Funding acquisition, Project administration, Resources, Validation, Writing – original draft, Writing – review & editing.

Declaration of Competing Interest

The authors declare that they have no known competing financial interests or personal relationships that could have appeared to influence the work reported in this paper.

Data availability

Data will be made available on request.

Acknowledgements

This work was supported by the “Crystallisation in the Real World” programme grant (EPSRC Grant number EP/R018820/1).

Appendix A. Supplementary data

Supplementary data to this article can be found online at https://doi.org/10.1016/j.jcrysgro.2022.126978.

References

[1] H. Du, E. Amstad, Angew. Chimie Int. Ed. 59 (2020) 1787-1816.
[2] D. Gebauer, A. Volkel, H. Colfen, Science 322 (2008) 1819–1822.
[3] A.F. Wallace, J.J. DeYoreo, P.M. Dove, J. Am. Chem. Soc. 131 (2009) 5244–5250.
[4] Q. Hu, M.H. Nielsen, C.L. Freeman, L. M. Hamm, J. Tao, J.R.I. Lee, T.Y.J. Han, U. Becker, J.H. Harding, P.M. Dove and J.J. De Yoreo, Faraday Discuss. 159, (2012) 509–523.
[5] A.F. Wallace, L.O. Hedges, A. Fernandez-Martinez, P. Raiteri, J.D. Gale, G.A. Waychunas, S. Whitelam, J.F. Banfield, J.J. De, Yoreo Science 341 (2013) 885-889.
[6] Z. Zou, W.J.E.M. Habraken, L. Bertinetti, Y. Politi, A. Gal, S. Weiner, L. Addadi, P. Fratzl, Adv. Mat. Int. (2016) 1600076.
[7] P.J.M. Smeets, A.R. Finney, W.J.E.M. Habraken, F. Nudelman, H. Friedrich, J. Laven, J.J. De Yoreo, P.M. Rodger, N.A.J.M. Sommerdijk, P.N.A.S. 114 (2017) E7882-E7890.
[8] D. Gebauer, M. Kellermeier, J.D. Gale, L. Bergström, H. Cölfen, Chem. Soc. Rev. 43 (2014) 2348–2371.
[9] J.J. De Yoreo, P.G. Vekilov, Rev. Mineral. Geochem. 54 (2003) 57–93.
[10] Z. Liu, Z. Zhang, Z. Wang, B. Jin, D. Li, J. Tao, R. Tang and J.J. De Yoreo, P.N.A.S. 117 (2020) 3397-3404.
[11] P. Bots, L.G. Benning, J.-D. Rodriguez-Blanco, T. Roncal-Herrero, S. Shaw, Cryst. Growth Des. 12 (2012) 3806–3814.
[12] J. Cavanaugh, M.L. Whittaker, D. Joester, Chem. Sci. 10 (2019) 5039–5043.
[13] A.J. Giuffre, A.C. Gagnon, J.J. De Yoreo, P.M. Dove Geo, Cosmo Acta 165 (2015) 407–417.
[14] M.H. Nielsen, S. Aloni, J.J. De Yoreo, Science 345 (2014) 1158–1162.
[15] J. Ihli, W.C. Wong, E.H. Noel, Yi-Yeoun Kim, A.N. Kulak, H.K. Christenson, M.J. Duer, F.C. Meldrum, Nat. Comm. (2014) 4169.
[16] M.P. Schmidt, A.J. Ilott, B.L. Phillips, R.J. Reeder, Cryst. Growth Des. 14 (2014) 938–951.
[17] A.V. Radha, A. Navrotsky, Crys. Grow. Des. 15 (2014) 70–78.
[18] H. Du, M. Steinacher, C. Borca, T. Huthwelker, A. Murello, F. Stellacci, E. Amstad, J. Am. Chem. Soc. 140 (2018) 14289–14299.
[19] J.M. Walker, B. Marzec, F. Nudelman, Angew. Chem. Int. Ed. 56 (2017) 11740–11743.
[20] E.M. Pouget, P.H.H. Bomans, J.A.C.M. Goos, P.M. Frederik, G. de With, N.A.J. M. Sommerdijk, Science 323 (2009) 1455–1458.
[21] T. Massa, A.J. Giuffre, C.-Y. Sun, C.A. Stifler, M.J. Frazier, M. Neder, N. Tamura, C. V. Stan, M.A. Marcus, P.U.P.A. Gilbert, P. N. A. S. 114 (2017) 7670–7678.

[22] M. Albéric, L. Bertinetti, Z. Zou, P. Fratzl, W. Habraken, Y. Politi, Adv. Sci. 5 (2018) 1701000.
[23] R.J. Reeder, Y. Tang, M.P. Schmidt, L.M. Kubista, D.F. Cowan, B.L. Phillips, Cryst. Growth Des. 13 (2013) 1905–1914.
[24] R. Innocenti Malini, Y.G. Bushuev, S.A. Hall, C.L. Freeman, P.M. Rodger, J.H. Harding, CrysEngComm. 18, (2016) 92-101.
[25] A. Carino, A. Testino, M.R. Andalibi, F. Pilger, P. Bowen, C. Ludwig, Cryst. Growth Des. 17 (2017) 2006–2015.
[26] P.G. Vekilov Cryst. Growth Des. **7,** (2007) 2796-2810.
[27] G.C. Sosso, J. Chen, S.J. Cox, M. Fitzner, P. Pedevilla, A. Zen, A. Michaelides Chem. Rev. 116**,** (2016) 7078-711.
[28] S. Karthica, T.K. Radhakrishnan, P. Kalaichelvi, Cryst. Growth Des. 16 (2016) 6663–6681.
[29] R. Darkins, I.J. McPherson, I.J. Ford, D.M. Duffy, P.R. Unwin, Cryst. Growth Des. 22 (2022) 982–986.
[30] H.-W. Wang, K. Yuan, N. Rampal, A.G. Stack, Cryst. Growth Des. 22 (2022) 853–870.
[31] A.E. Nielsen, J. Crys Grow. 67 (1984) 289–310.
[32] J.W.P. Schmelzer, J. Non-Crys. Solids 356 (2010) 2901–2907.
[33] W. Smith, T.R. Forester, J. Mol. Graphics 14 (1996) 136–141.
[34] P. Raiteri, J.D. Gale, J. Am. Chem. Soc. 132 (49) (2010) 17623–17634.
[35] L. Martínez, R. Andrade, E.G. Birgin, J.M. Martínez, Packmol J. Comput. Chem. 30 (13) (2009) 2157–2164.
[36] S.R. Yeandel, C.L. Freeman, J.H. Harding, J. Chem. Phys. in press.
[37] P. Fenter, Z. Zhang, C. Park, N.C. Sturchio, X.M. Hu, S.R. Higgins Geochim. et Cosmochim. Acta 71, (2007) 566–579.
[38] S. Kerisit, S.C. Parker, Chem. Commun. (2004) 52–53.
[39] M. Perez, M. Dumont, D. Acevedo-Reyes, Acta Materialia 56 (2008) 2119–2132.
[40] E. Clouet, M. Nastar, Phys. Rev. B 75 (2007), 132102.